

1  
2  
3  
4  
5  
6  
7  
8  
9  
10  
11  
12  
13  
14  
15  
16  
17  
18  
19  
20  
21  
22  
23  
24  
25  
26  
27  
28  
29  
30  
31  
32  
33  
34  
35  
36

TMT-based proteomic analysis of the antibiotic effects of ShangKeHuangShui against

*Staphylococcus aureus*.

Lichu Liu<sup>1¶\*</sup>, Na Zhao<sup>1¶</sup>, Kuangyang Yang<sup>1&\*</sup>, Honghong Liao<sup>&1</sup>, Xiaofang Liu<sup>1</sup>, Ying Wu<sup>2</sup>, Lei Lei<sup>2</sup>, Xiao Peng<sup>1</sup>, Yuanyan Wu<sup>1</sup>

<sup>1</sup>Institute of Orthopedics and Traumatology, Foshan Hospital of Traditional Chinese Medicine, Foshan, Guangdong, China

<sup>2</sup>Laboratory Medicine Center, Foshan Hospital of Traditional Chinese Medicine, Foshan, Guangdong, China

\*Corresponding author

E-mail:

[750691936@qq.com](mailto:750691936@qq.com) (LL)

[dr.yky@163.com](mailto:dr.yky@163.com) (KY)

¶These authors contributed equally to this work.

&These authors also contributed equally to this work.

## 37     **Abstract**

38     Post-traumatic infection is a serious orthopedic trauma complication commonly  
39     caused by *Staphylococcus aureus* (SAU). ShangKeHuangShui, also known as Yellow  
40     Aqueous Concentrate of Traumatology Herbs (YACTH), is prepared from six  
41     Chinese herbal medicines, which has been used for decades in our hospital to prevent  
42     post-traumatic infection.

43             In the present study, we investigated the *in vitro* antibacterial effects and  
44     underlying mechanism of YACTH against SAU. YACTH exhibited significant  
45     antibacterial activity against SAU with the minimum inhibitory concentration (MIC)  
46     of 8.625 mg/mL. Proteomic analysis based on Tandem mass tag (TMT) showed  
47     different protein expression levels in SAU under the YACTH and control conditions.  
48     Compared to the control group, the expression level of 490 proteins of YACTH  
49     treated group significantly changed (>1.2 fold, P <0.05). Biological informatics  
50     analysis showed that these differential proteins were widely involved in a variety of  
51     biological processes and multiple metabolic pathways. We then selected 26 target  
52     proteins to further conduct Parallel reaction monitoring (PRM). The results revealed  
53     that the 9 down-regulated proteins were mainly involved in RNA polymerase,  
54     oxidative phosphorylation, ABC transporter and glycolysis; whereas, the 17 up-  
55     regulated proteins are related to RNA degradation, mismatch repair and ribosome.

56             In conclusion, YACTH, which contains the water-soluble components of six  
57     Chinese herbs, is first reported to exhibit antibacterial activity against SAU *in vitro*.  
58     The results provide novel insights into the antibacterial mechanisms of YACTH on  
59     protein networks, which may help us find new potential antibiotic targets.

60

## 61 **Introduction**

62 *Staphylococcus aureus* (SAU), one species of coagulase Gram-positive  
63 staphylococcus, is widely found in the skin of mammals [1]. Due to its infectiousness  
64 and resistance to high temperature [2], SAU has become a major nosocomial  
65 pathogenic cause of superficial lesions, systemic infections, and several toxemic  
66 syndromes [3]. Skin injuries with open wounds can be easily infected by SAU and  
67 result in impetigo and folliculitis [4]. Infection with SAU is a serious complication for  
68 orthopedics trauma and is quite common in open fracture management [5].

69 To date, a variety of antibiotics have been invented to fight against SAU  
70 infection. Yellow Aqueous Concentrate of Traumatology Herbs (YACTH) is  
71 developed by six Chinese herbal medicines including Coptis Chinensis, Philodendron  
72 Chinensis, Gardenia jasminoides, Lithospermum, peppermint, and alum [6]. Its water-  
73 soluble components of berberine, geniposide, palmatine, and Phellodendron are  
74 potential natural antibacterial compounds that are reported to reduce subside swelling,  
75 invigorate blood circulation, promote tissue regeneration and improve wound healing  
76 [7,8]. However, whether such improvement was achieved by anti-inflammatory or  
77 antibacterial effects remained unknown, as well as the relevant molecular mechanism.  
78 In the presence of microorganisms, soft tissue injury and the consequent decline of  
79 antibacterial capability are the main causes of infection [9]. Considering YACTH  
80 contains antibacterial components, suggested that YACTH may promote wound  
81 healing through suppressing bacterial activities. Typically, the single component  
82 chemical compound, such as beta-lactam antibiotics inhibit SAU through bifunctional  
83 transglycosylase-transpeptidases PBP [10] and tetracyclines that bind to the 30S  
84 subunit of the ribosome to interfere with the protein synthesis of SAU [11], solely  
85 have one molecular target. Previous studies provided many antibiotics with clear

86 mechanisms. The majority of those antibiotics suppress SAU through targeting the  
87 cell envelope and proteins that are involved in protein synthesis and nucleic acids  
88 biosynthesis [12].

89 YACTH, as a compound formulation containing numbers of active antibacterial  
90 components, might have multi-target antibacterial activities, which makes it difficult  
91 to study the mechanism of how YACTH inhibits SAU. Proteomics is the analysis of  
92 the entire protein complement of a cell, tissue, or organism under a specific, defined  
93 set of conditions [13]. Up to date, proteomics could be applied to many fields due to  
94 the rapid development of technologies including protein fractionation techniques,  
95 mass spectrometry (MS) technology, bioinformatics, etc. The protein expression  
96 changes could be detected through MS, and reveal pathway information through  
97 informatics [14].

98 We hypothesized that YACTH inhibits SAU by regulating a variety of biological  
99 processes and multiple metabolic pathways. In the present study, we employed  
100 proteomics analysis to provide novel insights into the antibacterial mechanisms of  
101 YACTH on protein networks and explore some potential antibiotic targets.

## 102 **Materials and methods**

### 103 **Evaluation of Antibacterial Activity of YACTH**

#### 104 **Strain and Culture Condition**

105 The strain *S.aureus* ATCC 25923 used in this study was kept in lab and cultured  
106 aerobically in broth medium ( Qingdao Hope Bio-Technology Co., Ltd ) on a  
107 shaking incubator at 250 rpm, 37 °C.

## 108 **Antibacterial Activity of YACTH**

109 Antibacterial activity of YACTH was tested according to the agar diffusion method as  
110 reported previously with slight modification [15]. The YACTH extracts were filtered  
111 through 0.22  $\mu\text{m}$  sterilizing filters. Briefly, 100  $\mu\text{L}$  bacterial suspension containing  
112  $10^6$  CFU/mL of SAU was evenly smeared on Mueller-Hinton agar plates. Oxford  
113 cups (outside diameter of about 8.0 mm) were placed on the plates. After 20 min, 80  
114  $\mu\text{L}$  of YACTH were added to the Oxford cups. Saline was used in parallel  
115 experiments as a negative control. The diameters of the inhibitory zones (DIZs) were  
116 measured after incubation of the plates at 37 °C for 24 h, which were expressed in  
117 millimeter (mm) and recorded as mean  $\pm$  standard deviation (SD). DIZ values less  
118 than 8 mm were considered as no inhibition zone (NIZ). All experiments were  
119 performed in triplicate.

## 120 **Determination of MIC and MBC**

121 Minimum inhibitory concentration (MIC) and minimum bactericide concentration  
122 (MBC) were determined by a micro-dilution test according to the method described  
123 by Jeong [16]. Studies were conducted according to the guidelines recommended by  
124 the Clinical and Laboratory Standards Institute (CLSI) [17]. Two-fold serial dilutions  
125 of YACTH were prepared in sterile broth media ranging from 0.54-34.5 mg/mL.  
126 Afterwards, 180  $\mu\text{L}$  of diluted YACTH was mixed with 20  $\mu\text{L}$  bacterial suspension  
127 (approximately  $10^7$  CFU/mL) in the 96-well plates. The negative control contained  
128 180  $\mu\text{L}$  diluted YACTH with 20  $\mu\text{L}$  0.9% NaCl. The plates were incubated at 37 °C  
129 for 24 h. The MIC was defined as the concentration at which the corresponding well  
130 showed no visible bacterial growth after incubation at 37 °C for 24 h. Afterwards, a  
131 subculture of 50  $\mu\text{L}$  from each well with no visible bacterial growth was directly

132 incubated onto the nutrient agar plate incubating at 37 °C for 24 h, and the lowest on  
133 centration at which there was no colony growth was defined as MBC.

## 134 **Biochemistry experiments**

### 135 **Protein extraction and digestion**

136 The proteins were lysed and extracted with SDT buffer (4% SDS, 100 mM Tris-HCl, 1  
137 mM DTT, pH 7.6), and then quantified with the BCA protein assay kit (Bio-Rad,  
138 USA). After trypsin digestion, the peptides of each sample were desalted and  
139 concentrated by vacuum centrifugation and reconstituted in formic acid (40,0.1%  
140 (v/v)).

### 141 **Filter-aided sample preparation (FASP Digestion)**

142 200 µg of proteins of each sample were treated with 30 µL SDT buffer (4% SDS, 100  
143 mM DTT, 150 mM Tris-HCl pH 8.0). Used UA buffer (8 M Urea, 150 mM Tris-HCl  
144 pH 8.0) to remove detergent, DTT, and other low-molecular-weight components by  
145 repeated ultrafiltration (Microcon units, 10 kD). Added 100 µL iodoacetamide (100  
146 mM IAA in UA buffer) to block reduced cysteine residues. Incubated the samples for  
147 30 min in a dark environment. Washed the filters with 100 µL UA buffer three times  
148 and then 100 µL 25mM NH<sub>4</sub>HCO<sub>3</sub> buffer twice. Digested protein suspensions with 4  
149 µg trypsin (Promega) in 40 µL 25 mM NH<sub>4</sub>HCO<sub>3</sub> buffer at 37 °C overnight. The  
150 resulting peptides were collected as a filtrate. The peptides of each sample were  
151 desalted on C18 Cartridges (Empore™ SPE Cartridges C18 (standard density), bed  
152 I.D. 7 mm, volume 3 mL, Sigma), concentrated by vacuum centrifugation and

153 reconstituted in 40  $\mu$ L of 0.1% (v/v) formic acid. Estimated the peptide content by

154 UV light spectral density at 280 nm ( extinctions coefficient= 1.1, 0.1% (g/L) ) .

## 155 **SDS-PAGE**

156 Mixed 20  $\mu$ g of protein for each sample with loading buffer (5X) and boiled it for 5

157 min. The proteins were separated on 12.5% SDS-PAGE gel (constant current 14 mA,

158 90 min), and stained by Coomassie Blue R-250.

## 159 **TMT Labeling**

160 Peptides (100  $\mu$ g) of each sample were labeled with TMT reagent according to the

161 manufacturer's instructions (Thermo Scientific).

## 162 **High pH Reversed-Phase Fractionation**

163 Labeled peptides were fractionated by High pH Reversed-Phase Peptide Fractionation

164 Kit (Thermo Scientific). The dried peptides were reconstituted and acidified with

165 0.1% TFA solution and loaded on the equilibrated, high-pH, reversed-phase

166 fractionation spin column. Peptides were attached to the hydrophobic resin under

167 aqueous conditions and desalted by water through low-speed centrifugation. Collected

168 10 fractions from the gradient elution of the attached peptides by increasing

169 acetonitrile concentrations under high-pH. Desalted the collected fractions on C18

170 Cartridges (Empore™ SPE Cartridges C18 (standard density), bed I.D. 7 mm, volume

171 3 mL, Sigma) and concentrated them by vacuum centrifugation.

## 172 **LC-MS/MS analysis**

173 Performed LC-MS/MS analysis on a Q Exactive mass spectrometer (Thermo  
174 Scientific) that was coupled to Easy nLC (Proxeon Biosystems, now Thermo Fisher  
175 Scientific) for 60 min. At a flow rate of 300 nL/min, the peptides were applied to a  
176 reverse phase trap column (Thermo Scientific Acclaim PepMap100, 100  $\mu\text{m}$ \*2 cm,  
177 nanoViper C18) connected to the C18-reversed phase analytical column (Thermo  
178 Scientific Easy Column, 10 cm long, 75  $\mu\text{m}$  inner diameter, 3  $\mu\text{m}$  resin) in buffer A  
179 (0.1% Formic acid) and separated with a linear gradient of buffer B (84% acetonitrile  
180 and 0.1% Formic acid). The mass spectrometer was operated in positive ion mode.  
181 MS data were acquired via the most abundant precursor ions from the survey scan  
182 (300–1800 m/z) for HCD fragmentation using a data-dependent top10 method  
183 dynamically. Set automatic gain control (AGC) target to 3e6 and maximum inject  
184 time to 10 ms with a dynamic exclusion duration of 40.0 s. Acquired survey scans at a  
185 resolution of 70,000 at m/z 200 and set resolution for HCD spectra to 17,500 at m/z  
186 200, and isolation width was 2 m/z. Normalized collision energy was 30 eV and the  
187 underfill ratio, which specifies the minimum percentage of the target value likely to  
188 be reached at maximum fill time, was defined as 0.1%. Ran the instrument with  
189 peptide recognition mode enabled.

## 190 **Identification and quantitation of proteins**

191 Searched the MS raw data for each sample using the MASCOT engine, Uniprot  
192 (Matrix Science, London, UK; version 2.2) embedded into Proteome Discoverer 1.4  
193 software for identification and quantitation analysis.



## 194 **Bioinformatic analysis**

### 195 **Cluster analysis**

196 Performed hierarchical clustering analysis through Cluster 3.0  
197 (<http://bonsai.hgc.jp/~mdehoon/software/cluster/software.htm>) and Java Treeview  
198 software (<http://jtreeview.sourceforge.net>) and selected Euclidean distance algorithm  
199 for similarity measure and average linkage clustering algorithm (clustering uses the  
200 centroids of the observations) for clustering.

### 201 **Subcellular localization**

202 A multi-class SVM classification system, CELLO (<http://cello.life.nctu.edu.tw/>), was  
203 used to predict protein subcellular localization.

### 204 **Domain annotation**

205 Search protein sequences via the InterProScan software. Identified protein domain  
206 signatures from the InterPro member database P fam.

### 207 **GO annotation**

208 Locally searched the protein sequences of the selected differentially expressed  
209 proteins using the NCBI BLAST+client software (NCBI-blast-2.2.28 ± win32.exe)  
210 and found homologue sequences on InterProScan. Mapped then gene ontology (GO)  
211 terms and annotated the sequences using the software program Blast2GO. Plotted the  
212 GO annotation results by R scripts.

## 213 **KEGG annotation**

214 Blasted the studied proteins against the online Kyoto Encyclopedia of Genes and  
215 Genomes (KEGG) database (<http://geneontology.org/>) to retrieve their KEGG  
216 orthology identifications. Subsequently mapped the matched proteins to pathways in  
217 KEGG.

## 218 **Enrichment analysis**

219 The whole quantified proteins were considered as background dataset. The  
220 enrichment analysis was applied based on Fisher's exact test. Further applied  
221 Benjamini- Hochberg correction for multiple testing to adjust derived p-values. Only  
222 considered functional categories and pathways with p-values under a threshold of 0.05  
223 as significant.

## 224 **Statistical Analysis**

225 Statistical analysis was conducted with two-tailed t-test. The P value was set  
226 at  $< 0.05$ . Fisher's exact test was used to calculate the P value compare the distribution  
227 of each GO classification or KEGG pathway in the target protein set and the total  
228 protein set, and the enrichment analysis of GO annotation or KEGG pathway  
229 annotation was performed on the target protein set.

230

## 231 **Results**

### 232 **Antibacterial Activity of YACTH**

233 The antibacterial activity of YACTH against SAU was measured by Oxford cup and

234 micro-dilution methods, diameters of inhibition zone (DIZ) were appreciated as  
235 follows: not sensitive (diameter  $\leq 8.0$  mm), moderately sensitive ( $8.0 < \text{diameter} \leq$   
236  $14.0$  mm), sensitive ( $14.0 < \text{diameter} \leq 20.0$  mm), and extremely sensitive  
237 (diameter  $>20.0$  mm) [15]. The mean of DIZ values was 28.04mm ( $\pm 0.94$  mm), and  
238 the corresponding MIC and MBC against SAU were 8.625 mg/mL and 17.25 mg/mL,  
239 respectively.

## 240 **LC-MS/MS Analysis**

241 In this study, the TMT technique was applied to analyze the proteomics of SAU  
242 treated with YACTH. The experimental procedure is illustrated in Fig 1.

### 243 **Fig 1. Experimental procedure of LC-MS/MS analysis.**

244 Fig 1 shows the experimental procedures of our study. The YACTH group was compared to  
245 the control group. Each group contained three samples and went through protein preparation,  
246 labeling, fractionation, LC-MS/MS, protein identification and quantification, and  
247 bioinformatic analysis.

248 In LC-MS/MS analysis, a total of 470327 products were detected on the  
249 spectrum with 63749 matched with recorded data. Among these fractionated products,  
250 a total of 23544 peptides were identified and 16490 were recognized as unique, while  
251 2583 proteins were quantified out of the 2605 identified proteins. Compared to the  
252 control group, the expression of 490 proteins was significantly affected by the  
253 treatment of YACTH ( $P < 0.05$ ), while other proteins remained to be unchanged.  
254 Among these proteins, 241 proteins were up-regulated and 249 proteins were down-  
255 regulated (Fig 2A). To confirm the regulatory effects of YACTH on the growth and  
256 metabolism of SAU, a cluster plot was constructed to demonstrate the significant  
257 difference in protein expression between the control group and the YACTH treatment  
258 group (Fig 2B).

259 **Fig 2. Volcano plot and heat map of SAU protein expressions under YACTH treatment.**

260 Fig 2A is the volcano plot of the proteins that were affected by the YACTH treatment. While  
261 the grey dots represent the proteins that remained unchanged, the red dots represent the  
262 upregulated proteins and the blue dots represent the down-regulated proteins in the presence  
263 of YACTH. Fig 2B is the heat map that depicts the proteins being influenced by YACTH  
264 treatment. Each column represents a group of proteins. The protein expression levels are  
265 normalized by log<sub>2</sub> and labeled in different colors. The up-regulated proteins are colored in  
266 red, and down-regulated proteins are colored in blue.

267 **Functional Analysis**

268 In sub-cellular localization analysis, 384 cytoplasmic proteins, 83 membrane proteins,  
269 and 87 extracellular proteins were identified (S1 Fig). In addition, we conducted  
270 domain analysis to match YACTH regulated proteins with acknowledged structural  
271 domains. The majority of structural domains could be found in the proteins affected  
272 by YACTH treatment (Fig 3A). Typical structural domains such as ABC transporter,  
273 LPXTG cell wall anchor motif, YSIRK type signal peptide, radical SAM superfamily,  
274 and B domain, etc were observed. To study the overall response of SAU in the  
275 presence of YACTH, we performed GO analysis to assign the individual protein  
276 expression changes into certain groups. Take the example of the Top 20 enriched Go  
277 terms, proteins with significant expression changes were grouped into six biological  
278 processes with the highest number of proteins belongs to the cellular amide metabolic  
279 process, eight molecular functions with the highest number of proteins belong to RNA  
280 binding, six cellular components with the number of proteins almost evenly  
281 distributed in each cellular component (Fig 3B).

282 **Fig 3. Domain analysis and GO analysis of the SAU proteins that were affected by the**  
283 **YACTH treatment.**

284 Fig 3A shows the top 20 proteins that were matched with structural domains from the protein  
285 data bank. The length of the blue bars represents the number of proteins. Fig 3B depicts the  
286 GO enrichment analysis of the top 20 proteins. The proteins were categorized by biological  
287 process (BP), molecular function (MF), and cellular component (CC). The p-value is  
288 represented by the color intensity. The more intense red color represents a lower p-value.

289 In addition, we performed KEGG pathway analysis, which indicated that  
290 YACTH treatment regulated the expression of abundant SAU proteins, which were  
291 widely involved in a variety of biological processes and multiple metabolic pathways  
292 (Fig 4). The size of the dots represents the number of changed proteins, and the  
293 biggest protein number belongs to the ribosome, which is the key organelle  
294 responsible for translational activities. Other vital pathways related to SAU growth  
295 and metabolism, such as RNA polymerase, aminoacyl-tRNA biosynthesis, pyruvate  
296 metabolism, and aminoacyl-tRNA biosynthesis, were also presented in our data (Fig  
297 4).

298 **Fig 4. KEGG Pathway analysis of the SAU proteins that were affected by the YACTH**  
299 **treatment.**

300 The proteins influenced by the YACTH treatment are assigned to different pathways, while  
301 the top 20 pathways are exhibited in Fig 4. Five grades (from 1 to 5) of the p-value, converted  
302 by  $-\log_{10}$ , were presented in colors while the size of the dots represents the number of  
303 proteins.

## 304 **PRM analysis**

305 According to the GO and KEGG analysis of TMT results, 26 target proteins were  
306 selected to conduct PRM analysis; 6 of these proteins were significantly down-  
307 regulated and 20 proteins up-regulated as shown in Table 1. The up-regulated and  
308 down-regulated trends of all proteins of TMT were consistent with that of PRM

309 analysis. For example, the DEAD-box RNA helicase *cshA* related to RNA  
310 degradation was up-regulated by 1.25-fold and 1.35-fold, while Putative DNA-  
311 directed RNA polymerase subunit delta related to RNA polymerase was down-  
312 regulated to 0.36 times and 0.07 times in TMT and PRM analysis, respectively. The  
313 up-regulated proteins were primarily involved in the pathways related to the  
314 ribosome, mismatch repair, aminoacyl-tRNA biosynthesis, and ABC transporter, etc.  
315 Three proteins associated with Mismatch repair were up-regulated 1.25-1.27 times.  
316 Six proteins in the ribosome, two proteins in ABC transporter, and one protein in  
317 glycolysis were also up-regulated. On other hand, the down-regulated proteins were  
318 mainly involved in the pathways related to RNA polymerase and the two-component  
319 system. At the same time, some pathways were regulated in both up-and down-  
320 directions. In glycolysis, three proteins were upregulated, while two proteins were  
321 down-regulated; in ABC transporter, two proteins were up-regulated, while three  
322 proteins were down-regulated. All the TMT results are statistically significant, and  
323 PRM analysis further confirmed the results of TMT (Table 1).

324 **Table 1 PRM analysis of SAU proteins that were affected by the YACTH treatment.**

Map Name	Protein Name		Gene Name	TMT		PRM
				Ratio YACTH/Control	TTEST YACTH/Control	Ratio YACTH/Control
Mismatch repair	A0A0E0VPG2	RecJ	ST398NM01_1699	1.27	0.027	1.46
	Q6GFF3	DNA ligase	ligA	1.25	0.025	1.29
	P64319	ATP-dependent DNA helicase PcrA	pcrA	1.25	0.01	1.33
RNA degradation	A0A077UMU7	DEAD-box ATP-dependent RNA helicase CshA	cshA	1.25	0.049	1.35
RNA polymerase	P66725	DNA-directed RNA polymerase subunit omega	rpoZ	0.67	0.045	0.23
	A0A5S9C4T9	Putative DNA-directed RNA polymerase subunit delta	rpoE	0.36	0.004	0.07
Ribosome	A7X5D9	50S ribosomal protein L18	rplR	1.81	0.016	1.94
	A0A033UZC9	30S ribosomal protein S21	rpsU	1.6	0.017	2.04
	A0A2D1CK30	30S ribosomal protein S10	rpsJ	1.45	0.001	1.57
	A0A077VMB7	50S ribosomal protein L21	rplU	1.42	0.032	1.38
	Q2YYQ1	50S ribosomal protein L22	rplV	1.39	0.009	2.57
	A0A0H2HWH9	50S ribosomal protein L14	rplN	1.24	0.036	1.83
	Q6GJC3	30S ribosomal protein S12	rpsL	0.81	0.041	0.45
Glycolysis	A0A0E0VRM3	Acetyl-coenzyme A synthetase	ST398NM01_1785	0.62	0.001	0.23

Oxidative phosphorylation	A0A0E1XGX4	Succinate dehydrogenase iron-sulfur subunit	sdhB	0.82	0.013	0.69
ABC transporters	A0A454GWW4	SAV1866 family putative multidrug efflux ABC transporter (Fragment)	C7P97_12990	1.26	0.012	3.09
	A0A0E1XEH6	Periplasmic binding protein	HMPREF0769_10977	1.25	0.049	1.71
	A0A0E1XHE1	ABC transporter, ATP-binding protein	HMPREF0769_11391	0.59	0	0.18
	A0A2X2K196	Response regulator ArlR	arlR_1	0.66	0.001	0.56
	Q6GFH6	Low molecular weight protein-tyrosine-phosphatase PtpA	ptpA	0.58	0.025	0.31
	A0A1Q8DED0	D-alanyl carrier protein	dltC	0.44	0.047	0.06

325 Table 1 shows the 26 affected proteins related to 7 biological processes & metabolic pathways. All the TMT results are statistically significant( $p < 0.05$ ) and are confirmed by

326 PRM analysis. The ratio of down-regulated proteins in YACTH group compared to the control group is highlighted in green.

327



## 328 **Discussion**

329 SAU is a gram-positive bacterium that causes many diseases [18], the current  
330 therapeutic strategies against SAU mainly target the cell envelope, protein synthesis,  
331 and nucleic acids biosynthesis of the bacteria [19]. With the extensive use  
332 of antibiotics, the emergence of drug-resistant strains has become a great challenge for  
333 their treatment, which urges people to explore new antibiotics [20]. The herbal  
334 formular of YACTH is widely used in Southern China to prevent post-traumatic  
335 infection which is commonly caused by SAU [21,22]. In the present study, proteomic  
336 analysis was used to analyze the effects of YACTH on the protein expression of SAU.  
337 The expressions of 490 proteins were significantly changed in YACTH treated group  
338 compared to the control group. These altered proteins were widely associated with a  
339 variety of biological processes and multiple metabolic pathways. Interestingly, the  
340 down-regulated proteins were mainly involved in the pathways related to RNA  
341 polymerase (RNAP), oxidative phosphorylation, and two-component system. The  
342 RNAP multisubunit complex is responsible for bacterial transcription [23]. It contains  
343  $\alpha$  (two copies),  $\beta$ ,  $\beta'$  and  $\omega$  subunit (Fig 5). The small  $\omega$  subunit, namely rpoZ, plays  
344 key roles in subunit folding, complex assembly, and maintenance of transcriptional  
345 integrity [24]. The  $\delta$  factor, rpoE, plays an essential role in RNA polymerase function  
346 in SAU [25]. The ablation of rpoE resulted in decreased transcription, protein  
347 synthesis, and pathogenicity [26]. The decreased expression of rpoZ and rpoE in SAU  
348 exposed to YACTH suggested that it may inhibit SAU's activities on transcription  
349 level by RNAP pathway. In addition, YACTH significantly increased the level of the  
350 DEAD-box RNA helicase cshA, which was responsible for RNA degradation and  
351 might regulate the expression of virulence factors [27].

352 **Figure 5. RNA polymerase of bacteria and eukaryote.**

353 YACTH significantly down-regulated the expression of several proteins in two-  
354 component system and oxidative phosphorylation pathways, including arlRs, ptpA,  
355 dltC, and sdhB, etc (Table1), which were potential antibiotics targets associated with  
356 bacterial virulence and biofilm formation of SAU [28,29]. The two-component system  
357 signal transduction plays a pivotal role in regulating virulence gene expression, cell  
358 wall synthesis, biofilm formation, by which bacteria adapt to the external environment  
359 [30]. The biofilm formation of SAU is closely related to the intercellular  
360 communication and self-defense of the bacteria against antibiotics [31]. For example,  
361 arlRs is an antibiotic target for oxacillin, deletion of the arlRs in SAU increased its  
362 susceptibilities to oxacillin [32]. The protein tyrosine phosphatase ptpA is a signaling  
363 molecule and may interfere with host cell signaling [29,33], which contributes to the  
364 infectivity of SAU [34]. Deletion of ptpA not only impaired the survival rates of SAU  
365 in macrophages but also reduce the SAU infectivity on mice [29]. DltC, a two-  
366 component system protein that affects the cell surface charge of bacteria, is involved  
367 in the D-alanine substitution of lipoteichoic acid, and therefore biofilm formation  
368 [35]. dltC regulates D-alanine incorporation into cell wall polymers in SAU. A lack of  
369 this decoration leads to increased susceptibility to cationic antimicrobial peptide  
370 [36,37]. Another downregulated protein associated with biofilm formation is sdhB, a  
371 succinate dehydrogenase iron-sulfur subunit involved in the oxidation  
372 phosphorylation pathway[38]. The sdhB gene knockout resulted in a 1.2 fold  
373 significant decrease of biofilm formation[39], while mutation of sdhB led to defect in  
374 the persistence of levofloxacin[38].

375 On other hand, the up-regulated proteins were primarily involved in the  
376 pathways related to mismatch repair, ribosome, aminoacyl-tRNA biosynthesis, and  
377 ABC transporter (Table 1). The up-regulated mismatch repair proteins included pcrA,

378 recJ, and ligA. ATP-dependent DNA helicase pcrA is an essential helicase in Gram-  
379 positive bacteria, genetic induction experiment indicated that overproduction of pcrA  
380 has deleterious effects on the host cell and plasmid replication [40]. Single-stranded-  
381 DNA-specific exonuclease recJ is involved in a variety of DNA repair pathways  
382 corresponding to their cleavage polarities, but the relationship between the cleavage  
383 polarity and the respective DNA repair pathways has not been clarified [41]. NAD-  
384 dependent DNA ligase (ligA) has been thought of as a potential broad-spectrum  
385 antibacterial target [42,43,44] and was later proved to be an antibacterial target of  
386 SAU and inhibited by pyridochromanone[42]. Our result suggested that YACTH  
387 impaired SAU and therefore led to stress response with increased expression of  
388 proteins that are involved in mismatch repair. For ribosomes, eighteen ribosomal  
389 proteins were upregulated, while only one ribosomal protein was downregulated in  
390 YACTH treatment group (table1). Among the 18 upregulated ribosomal proteins, four  
391 are related to antibiotics sensitivity, as was reported in previous publications.  
392 Mutations of 30S ribosomal proteins S21, rpsU, led to reduced susceptibility of  
393 vancomycin of SAU [45]. Increased level of rpIN was also observed in vancomycin-  
394 intermediate SAU (VISA) [46]. Mutations on 30S ribosomal proteins S10, rpsJ, was  
395 reported to be the cause of reduced tigecycline susceptibility [47]. While mutation of  
396 50S ribosomal protein L22, rplV, is related to several antibiotic resistance, high-level  
397 telithromycin selection led to the mutation on rplV [48], mutations of rplV reduced  
398 sensitivity of SAU to erythromycin and other macrolides were not only observed in  
399 the laboratory but also clinical studies [49,50,51].

400 As mentioned above, we reported a new antimicrobial herbal formularlation of  
401 YACTH and its effects on the expression of bacterial proteins, which might be an  
402 alternative choice to protect against post-traumatic infection caused by SAU. The

403 multiple proteins down-regulated by YACTH were primarily involved in the RNA  
404 polymerase, oxidative phosphorylation, and two-component system pathways, which  
405 are associated with the biofilm formation and the virulence secretion of SAU.  
406 Otherwise, up-regulated proteins by YACTH were mainly presented in the pathways  
407 of mismatch repair, ribosome aminoacyl-tRNA biosynthesis, and ABC transporter,  
408 etc. Some down- and up-regulated proteins were found to be related to antibiotic  
409 sensitivity. These results provided pieces of evidence for the hypothesis that YACTH  
410 might repress the growth and infectivity of SAU by either reducing or increasing the  
411 expression of target proteins. Some of these proteins were associated with cell  
412 envelope, protein synthesis, and nucleic acid biosynthesis, which are pathways that  
413 are targets of traditional antibiotics. Unlike common antibiotics that solely mediated  
414 on one specific target, YACTH regulated multiple proteins that are involved in several  
415 signaling pathways, probably due to its complex components. Such results provided a  
416 broad direction of exploring new anti-bacterial targets to fight against SAU. Further  
417 studies were needed to clarify the preliminary antibacterial mechanism of each  
418 effective component, structure, and potential targets.

#### 419 **Reference**

- 420 1. Wertheim HF, Melles DC, Vos MC, van Leeuwen W, van Belkum A, Verbrugh  
421 HA, et al. The role of nasal carriage in *Staphylococcus aureus* infections. *Lancet*  
422 *Infect Dis.* 2005;5(12):751-62. doi: 10.1016/S1473-3099(05)70295-4.
- 423 2. Sabike II, Fujikawa H, Sakha MZ, Edris AM. Production of *Staphylococcus*  
424 *aureus* enterotoxin a in raw milk at high temperatures. *J Food Prot.*  
425 2014;77(9):1612-6. doi: 10.4315/0362-028X.JFP-13-527.
- 426 3. Aggarwal S, Jena S, Panda S, Sharma S, Dhawan B, Nath G, et al. Antibiotic  
427 susceptibility, virulence pattern, and typing of *Staphylococcus aureus* strains  
428 Isolated from variety of infections in India. *Front Microbiol.* 2019;10:2763. doi:  
429 10.3389/fmicb.2019.02763.
- 430 4. Nowicka D, Grywalska E. *Staphylococcus aureus* and host immunity in recurrent  
431 furunculosis. *Dermatology.* 2019;235(4):295-305. doi: 10.1159/000499184. Epub  
432 2019 Apr 17.
- 433 5. Yang L, Feng J, Liu J, Yu L, Zhao C, Ren Y, et al. Pathogen identification in 84  
434 Patients with post-traumatic osteomyelitis after limb fractures. *Ann Palliat Med*  
435 2020;9(2):451-458. doi: 10.21037/apm.2020.03.29
- 436 6. Li Z, Zheng F, C Y, Li H, Liu D, Liu X. Optimization of the preparation process

- 437 of Shangkehuangshui II. *ChinHospPharmJ*, 2018;38(24):2532-  
438 36. doi:10.13286/J.cnki.chinhosppharmacyj.2018.24.07
- 439 7. Xu H, Li Z, Lei K, Li H, Liu D, Chen Y, et al. Study on the effect of  
440 Shangkehuangshui on acute soft tissue injury. *Pharmacology and clinic of*  
441 *traditional Chinese medicine* 2017; 33 (6): 124-130
- 442 8. Cai L, Yang H, Sun B, Wen J, WuF, Wu F, Y J. Effect of the traumatology  
443 yellow water on new bone formation of distraction osteogenesis zone in rabbit.  
444 *Bone Setting of Traditional Chinese medicine*. 2014; 26 (10): 12-15.
- 445 9. Källicke T, Schlegel U, Printzen G, Schneider E, Muhr G, Arens S. Influence of a  
446 standardized closed soft tissue trauma on resistance to local infection. An  
447 experimental study in rats. *J Orthop Res*. 2003, 21(2):373-8. doi: 10.1016/S0736-  
448 0266(02)00149
- 449 10. Giesbrecht P, Kersten T, Maidhof H et al. Staphylococcal cell  
450 wall:morphogenesis and fatal variations in the presence of penicillin. *Microbiol*  
451 *Mol Biol R* 1998;62:1371-41
- 452 11. Nguyen F, Starosta AL, Arenz S et al. Tetracycline antibiotics and resistance  
453 mechanisms. *Biol Chem* 2014;395:559-75.
- 454 12. Foster TJ. Antibiotic resistance in *Staphylococcus aureus*. Current status and  
455 future prospects. *FEMS Microbiol Rev*. 2017 May 1;41(3):430-449.
- 456 13. Schulze WX, Usadel B. Quantitation in mass-spectrometry-based proteomics.  
457 *Annu Rev Plant Biol*. 2010;61:491-516.
- 458 14. Aebersold R, Burlingame AL, Bradshaw RA. Western blots versus selected  
459 reaction monitoring assays: time to turn the tables? *Mol Cell Proteomics*. 2013  
460 Sep;12(9):2381-2. doi: 10.1074/mcp.E113.031658.
- 461 15. Cao J, Fu H, Gao L, Zheng Y. Antibacterial activity and mechanism of  
462 lactobionic acid against *Staphylococcus aureus*. *Folia Microbiol (Praha)*. 2019  
463 Nov;64(6):899-906
- 464 16. Jeong YI, Na HS, Seo DH, Kim DG, Lee HC, Jang MK, et al. Ciprofloxacin-  
465 encapsulated poly(DL-lactide-co-glycolide) nanoparticles and its antibacterial  
466 activity. *Int J Pharm*. 2008 Mar 20;352(1-2):317-23. doi:  
467 10.1016/j.ijpharm.2007.11.001.
- 468 17. CLSI Guidelines (2018) Performance Standards for Antimicrobial Susceptibility  
469 Testing. 28th Edition (M100S).
- 470 18. Oliveira D, Borges A, Simões M. *Staphylococcus aureus* Toxins and Their  
471 Molecular Activity in Infectious Diseases. *Toxins (Basel)*. 2018 Jun  
472 19;10(6):252. doi: 10.3390/toxins10060252.
- 473 19. Assis LM, Nedeljković M, Dessen A. New strategies for targeting and treatment  
474 of multi-drug resistant *Staphylococcus aureus*. *Drug Resist Updat*. 2017  
475 Mar;31:1-14. doi: 10.1016/j.drug.2017.03.001.
- 476 20. Brown ED, Wright GD. Antibacterial drug discovery in the resistance era.  
477 *Nature*. 2016 Jan 21;529(7586):336-43. doi: 10.1038/nature17042. PMID:  
478 26791724.
- 479 21. Helmann JD. RNA polymerase: a nexus of gene regulation. *Methods*. 2009  
480 Jan;47(1):1-5. doi: 10.1016/j.ymeth.2008.12.001. PMID: 19070783; PMCID:  
481 PMC3022018.
- 482 22. Weiss A, Shaw LN. Small things considered: the small accessory subunits of  
483 RNA polymerase in Gram-positive bacteria. *FEMS Microbiol Rev*. 2015  
484 Jul;39(4):541-54. doi: 10.1093/femsre/fuv005.
- 485 23. Mathew R, Chatterji D. The evolving story of the omega subunit of bacterial  
486 RNA polymerase. *Trends Microbiol*. 2006 Oct;14(10):450-5. doi:

- 487 10.1016/j.tim.2006.08.002.
- 488 24. Weiss A, Moore BD, Tremblay MHJ, Chaput D, Kremer A, Shaw LN. The  $\omega$   
489 subunit governs RNA polymerase stability and transcriptional specificity in  
490 *Staphylococcus aureus*. *J Bacteriol.* 2016 Dec 28;199(2):e00459-16. doi:  
491 10.1128/JB.00459-16. PMID: 27799328; PMCID: PMC5198492.
- 492 25. Lin Z, Wang F, Shang Z, Lin W. Biochemical and structural analyses reveal  
493 critical residues in  $\delta$  subunit affecting its bindings to  $\beta'$  subunit of *Staphylococcus*  
494 *aureus* RNA polymerase. *Biochem Biophys Res Commun.* 2021 Mar 19;545:98-  
495 104. doi: 10.1016/j.bbrc.2021.01.078.
- 496 26. Weiss A, Ibarra JA, Paoletti J, Carroll RK, Shaw LN. The  $\delta$  subunit of RNA  
497 polymerase guides promoter selectivity and virulence in *Staphylococcus aureus*.  
498 *Infect Immun.* 2014 Apr;82(4):1424-35. doi: 10.1128/IAI.01508-14.
- 499 27. Oun S, Redder P, Didier JP, François P, Corvaglia AR, Buttazzoni E, Giraud C,  
500 Girard M, Schrenzel J, Linder P. The CshA DEAD-box RNA helicase is  
501 important for quorum sensing control in *Staphylococcus aureus*. *RNA Biol.* 2013  
502 Jan;10(1):157-65. doi: 10.4161/rna.22899.
- 503 28. Horn J, Stelzner K, Rudel T, Fraunholz M. Inside job: *Staphylococcus aureus*  
504 host-pathogen interactions. *Int J Med Microbiol.* 2018 Aug;308(6):607-624. doi:  
505 10.1016/j.ijmm.2017.11.009. Epub 2017 Nov 26. PMID: 29217333.
- 506 29. Gannoun-Zaki L, Pätzold L, Huc-Brandt S, Baronian G, Elhaway MI, Gaupp R, et  
507 al. PtpA, a secreted tyrosine phosphatase from *Staphylococcus aureus*, contributes  
508 to virulence and interacts with coronin-1A during infection. *J Biol Chem.* 2018  
509 Oct 5;293(40):15569-15580. doi:10.1074/jbc.RA118.003555.
- 510 30. Kuroda M, Ohta T, Uchiyama I, Baba T, Yuzawa H, Kobayashi I, et al. Whole  
511 genome sequencing of methicillin-resistant *Staphylococcus aureus*. *Lancet.* 2001  
512 Apr 21;357(9264):1225-40. doi: 10.1016/s0140-6736(00)04403-2.
- 513 31. Schilcher K, Horswill AR. Staphylococcal biofilm development: structure,  
514 regulation, and treatment strategies. *Microbiol Mol Biol Rev.* 2020 Aug  
515 12;84(3):e00026-19. doi: 10.1128/MMBR.00026-19.
- 516 32. Bai J, Zhu X, Zhao K, Yan Y, Xu T, Wang J, et al. The role of ArlRS in  
517 regulating oxacillin susceptibility in methicillin-resistant *Staphylococcus aureus*  
518 indicates it is a potential target for antimicrobial resistance breakers. *Emerg*  
519 *Microbes Infect.* 2019;8(1):503-515. doi: 10.1080/22221751.2019.1595984.
- 520 33. Brelle S, Baronian G, Huc-Brandt S, Zaki LG, Cohen-Gonsaud M, Bischoff M, et  
521 al. Phosphorylation-mediated regulation of the *Staphylococcus aureus* secreted  
522 tyrosine phosphatase PtpA. *Biochem Biophys Res Commun.* 2016 Jan  
523 15;469(3):619-25. doi: 10.1016/j.bbrc.2015.11.123. Epub 2015 Dec 8.
- 524 34. Vega C, Chou S, Engel K, Harrell ME, Rajagopal L, Grundner C. Structure and  
525 substrate recognition of the *Staphylococcus aureus* protein tyrosine phosphatase  
526 PtpA. *J Mol Biol.* 2011 Oct 14;413(1):24-31. doi: 10.1016/j.jmb.2011.08.015.
- 527 35. Matsuo M, Oogai Y, Kato F, Sugai M, Komatsuzawa H. Growth-phase  
528 dependence of susceptibility to antimicrobial peptides in *Staphylococcus aureus*.  
529 *Microbiology (Reading).* 2011 Jun;157(Pt 6):1786-1797. doi:  
530 10.1099/mic.0.044727-0.
- 531 36. Reichmann NT, Cassona CP, Gründling A. Revised mechanism of D-alanine  
532 incorporation into cell wall polymers in Gram-positive bacteria. *Microbiology*  
533 *(Reading).* 2013 Sep;159(Pt 9):1868-1877. doi: 10.1099/mic.0.069898-0.
- 534 37. Wood BM, Santa Maria JP Jr, Matano LM, Vickery CR, Walker S. A partial  
535 reconstitution implicates DltD in catalyzing lipoteichoic acid d-alanylation. *J Biol*  
536 *Chem.* 2018 Nov 16;293(46):17985-17996. doi: 10.1074/jbc.RA118.004561.

- 537 38. Wang W, Chen J, Chen G, Du X, Cui P, Wu J, et al. Transposon mutagenesis  
538 identifies novel genes associated with *Staphylococcus aureus* persister formation.  
539 *Front Microbiol.* 2015 Dec 23;6:1437. doi: 10.3389/fmicb.2015.01437.
- 540 39. De Backer S, Sabirova J, De Pauw I, De Greve H, Hernalsteens JP, Goossens  
541 H, et al. Enzymes catalyzing the *tca*- and urea cycle influence the matrix  
542 composition of biofilms formed by methicillin-resistant *Staphylococcus aureus*  
543 USA300. *Microorganisms.* 2018 Oct 29;6(4):113. doi:  
544 10.3390/microorganisms6040113.
- 545 40. Iordanescu S. Characterization of the *Staphylococcus aureus* chromosomal gene  
546 *pcrA*, identified by mutations affecting plasmid pT181 replication. *Mol Gen*  
547 *Genet.* 1993 Oct;241(1-2):185-92. doi: 10.1007/BF00280216.
- 548 41. Shimada A, Masui R, Nakagawa N, Takahata Y, Kim K, Kuramitsu S, et al. A  
549 novel single-stranded DNA-specific 3'-5' exonuclease, *Thermus thermophilus*  
550 exonuclease I, is involved in several DNA repair pathways. *Nucleic Acids Res.*  
551 2010 Sep;38(17):5692-705. doi: 10.1093/nar/gkq350.
- 552 42. Dwivedi N, Dube D, Pandey J, Singh B, Kukshal V, Ramachandran R, et al.  
553 NAD(+)-dependent DNA ligase: a novel target waiting for the right inhibitor.  
554 *Med Res Rev.* 2008 Jul;28(4):545-68. doi: 10.1002/med.20114.
- 555 43. Podos SD, Thanassi JA, Pucci MJ. Mechanistic assessment of DNA ligase as an  
556 antibacterial target in *Staphylococcus aureus*. *Antimicrob Agents Chemother.*  
557 2012 Aug;56(8):4095-102. doi: 10.1128/AAC.00215-12.
- 558 44. Kaczmarek FS, Zaniewski RP, Gootz TD, Danley DE, Mansour MN, Griffor M,  
559 et al. Cloning and functional characterization of an NAD(+)-dependent DNA  
560 ligase from *Staphylococcus aureus*. *J Bacteriol.* 2001 May;183(10):3016-24. doi:  
561 10.1128/JB.183.10.3016-3024.2001.
- 562 45. Blake KL, O'Neill AJ. Transposon library screening for identification of genetic  
563 loci participating in intrinsic susceptibility and acquired resistance to  
564 antistaphylococcal agents. *J Antimicrob Chemother.* 2013 Jan;68(1):12-6. doi:  
565 10.1093/jac/dks373. Epub 2012 Oct 7.
- 566 46. Sirichoat A, Lulitanond A, Kanlaya R, Tavichakorntrakool R, Chanawong A,  
567 Wongthong S, et al. Phenotypic characteristics and comparative proteomics of  
568 *Staphylococcus aureus* strains with different vancomycin-resistance levels. *Diagn*  
569 *Microbiol Infect Dis.* 2016 Dec;86(4):340-344. doi:  
570 10.1016/j.diagmicrobio.2016.09.011.
- 571 47. Beabout K, Hammerstrom TG, Perez AM, Magalhães BF, Prater AG, Clements  
572 TP, et al. The ribosomal S10 protein is a general target for decreased tigecycline  
573 susceptibility. *Antimicrob Agents Chemother.* 2015 Sep;59(9):5561-6. doi:  
574 10.1128/AAC.00547-15.
- 575 48. Gentry DR, Holmes DJ. Selection for high-level telithromycin resistance in  
576 *Staphylococcus aureus* yields mutants resulting from an *rplB*-to-*rplV* gene  
577 conversion-like event. *Antimicrob Agents Chemother.* 2008 Mar;52(3):1156-8.  
578 doi: 10.1128/AAC.00923-07. Epub 2008 Jan 14.
- 579 49. Prunier AL, Malbruny B, Laurans M, Brouard J, Duhamel JF, Leclercq R. High  
580 rate of macrolide resistance in *Staphylococcus aureus* strains from patients with  
581 cystic fibrosis reveals high proportions of hypermutable strains. *J Infect Dis.* 2003  
582 Jun 1;187(11):1709-16. doi: 10.1086/374937.
- 583 50. Prunier AL, Malbruny B, Tandé D, Picard B, Leclercq R. Clinical isolates of  
584 *Staphylococcus aureus* with ribosomal mutations conferring resistance to  
585 macrolides. *Antimicrob Agents Chemother.* 2002 Sep;46(9):3054-6. doi:  
586 10.1128/aac.46.9.3054-3056.2002.

587 51. Han D, Liu Y, Li J, Liu C, Gao Y, Feng J, et al. Twenty-seven-nucleotide repeat  
588 insertion in the rplV gene confers specific resistance to macrolide antibiotics in  
589 Staphylococcus aureus. Oncotarget. 2018 May 25;9(40):26086-26095. doi:  
590 10.18632/oncotarget.25441.

## 591 **Supporting Information**

592 **S1 Fig. Subcellular localization of the SAU proteins that were affected by the YACTH**  
593 **treatment.**

594 The SAU proteins that were affected by YACTH treatment were assigned into three subcellular  
595 locations: cytoplasmic(384), extracellular(87), and membrane(83).



<https://doi.org/10.1101/2021.07.22.453437>; this version posted July 22, 2021. The copyright holder for this preprint (which was not certified by peer review) is the author/funder, who has granted bioRxiv a license to display the preprint in perpetuity. It is made available under aCC-BY 4.0 International license.

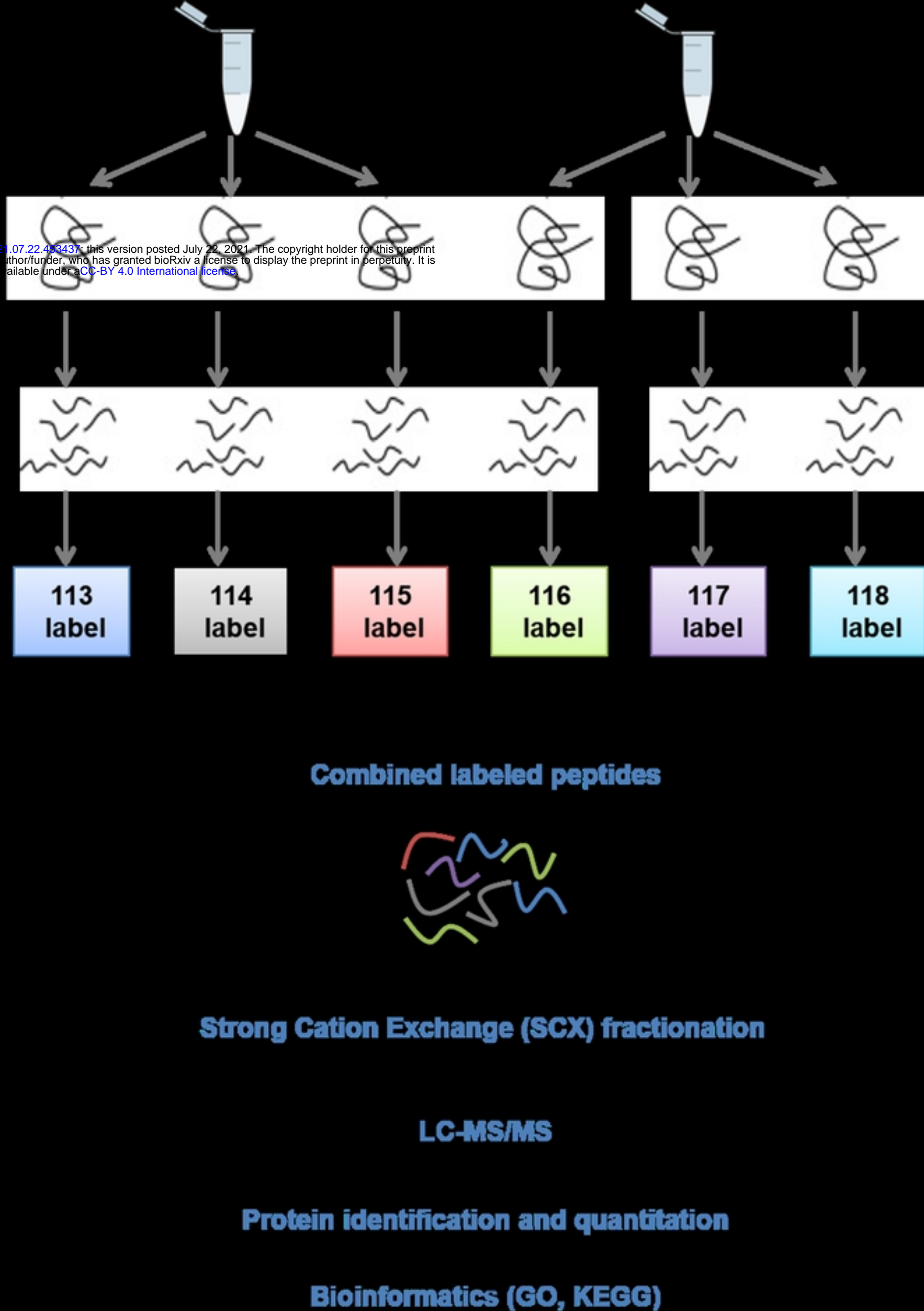


Fig 1

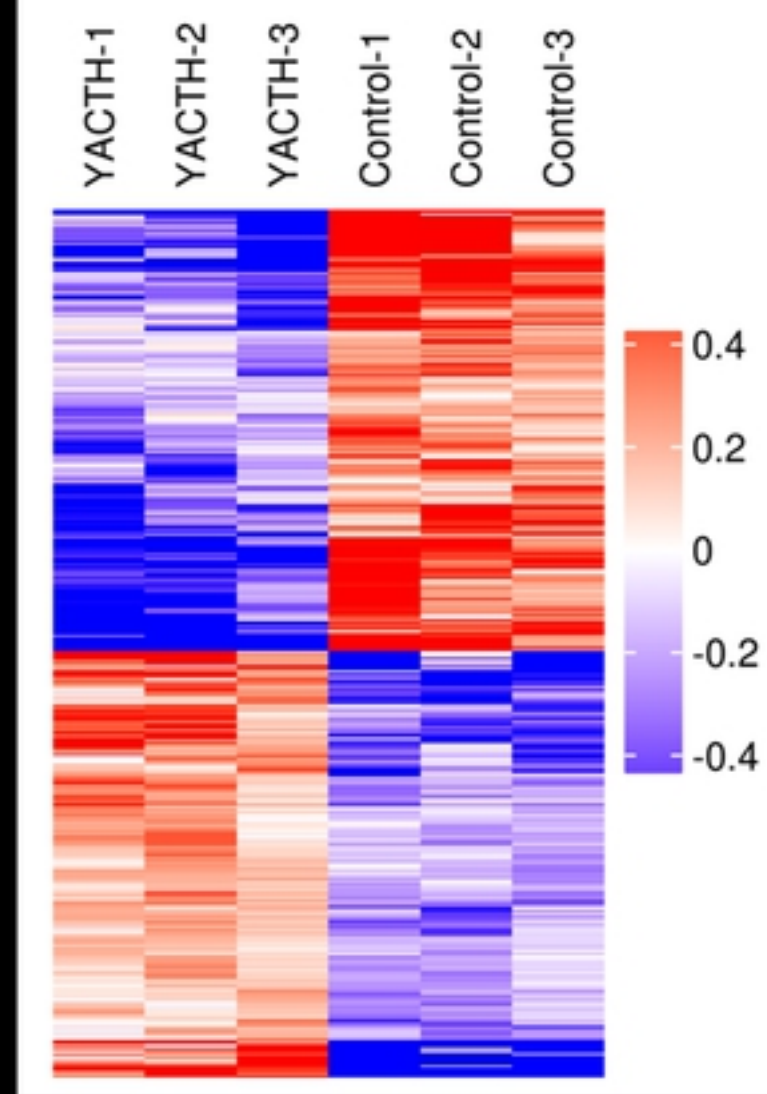
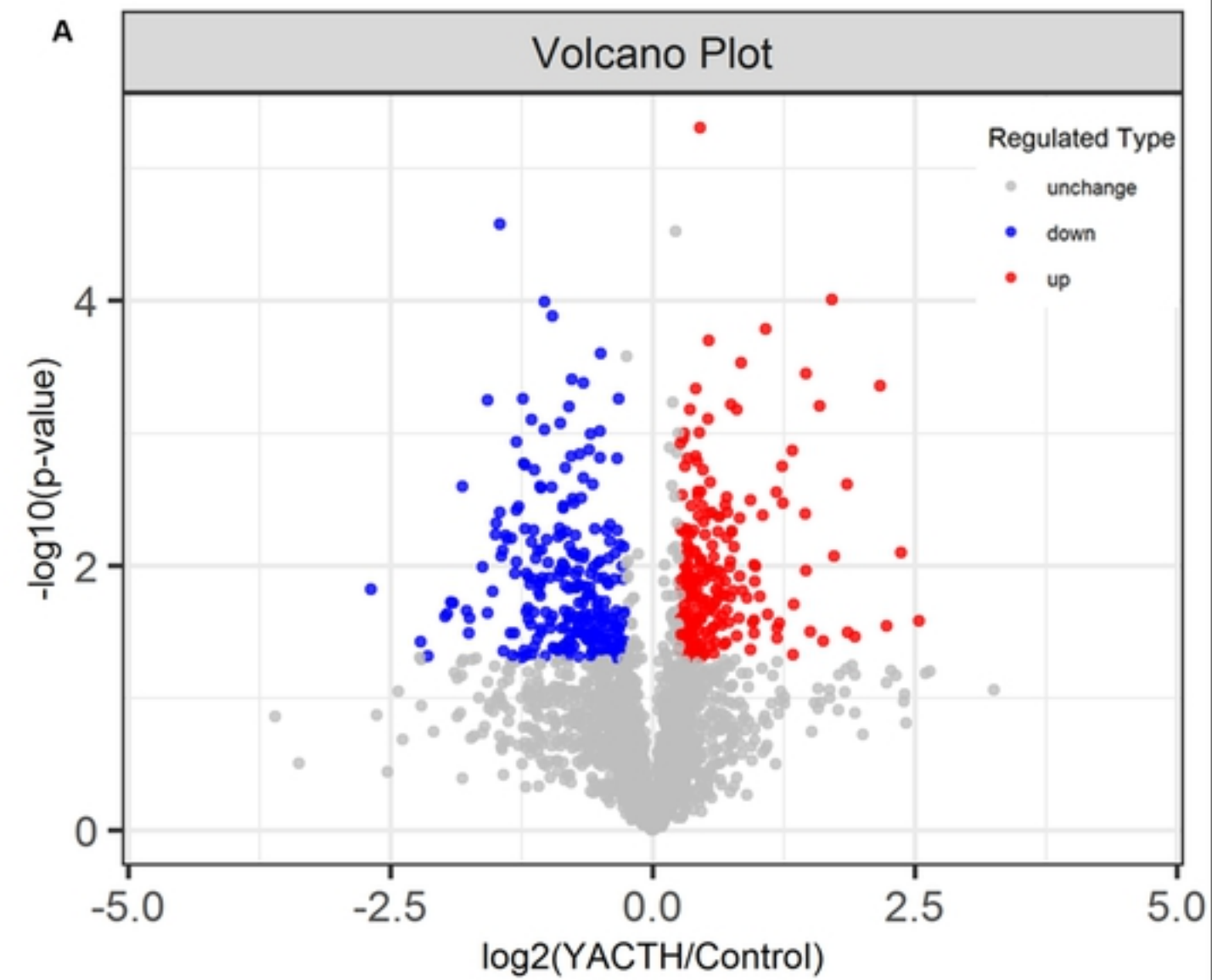


Fig 2

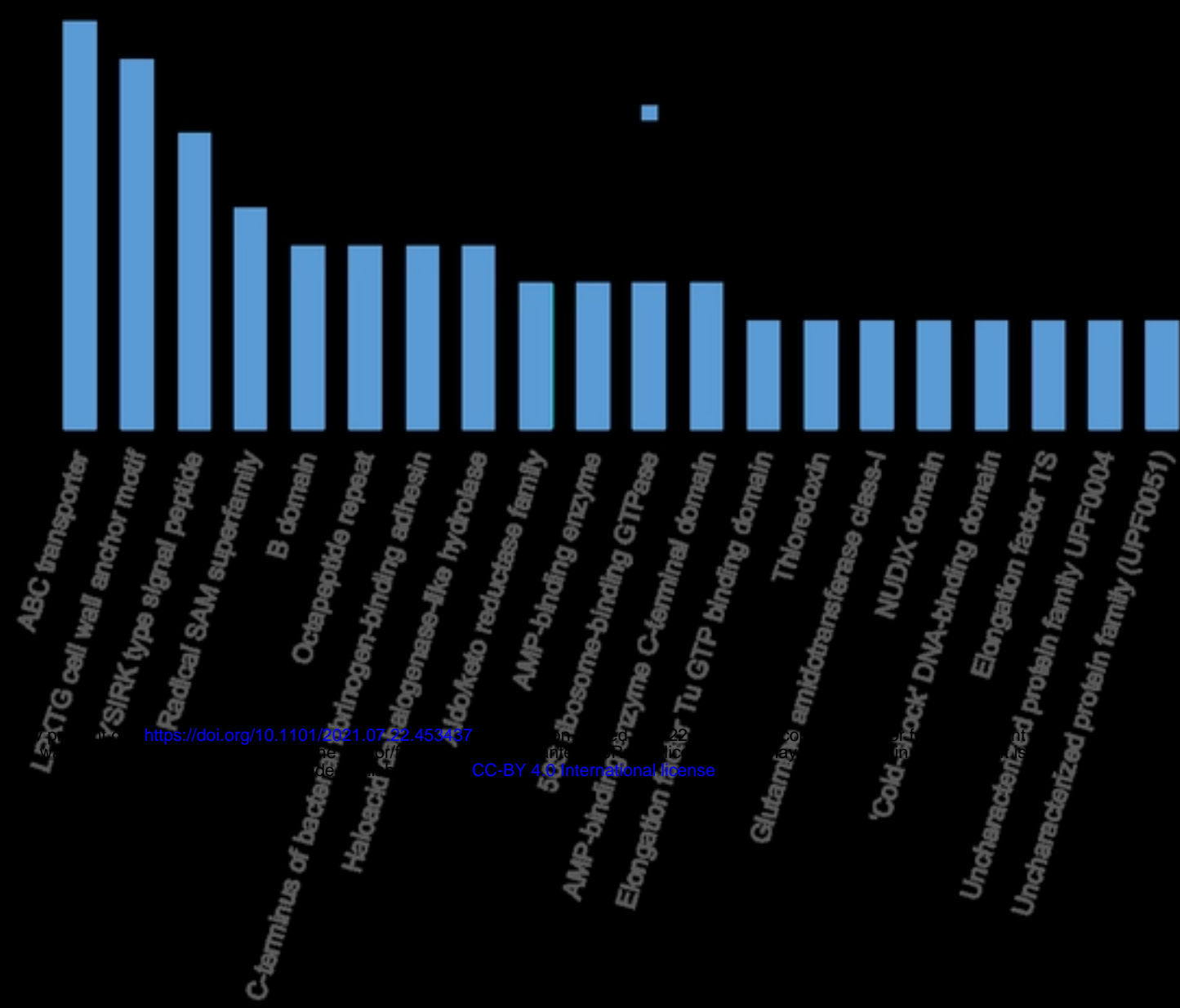
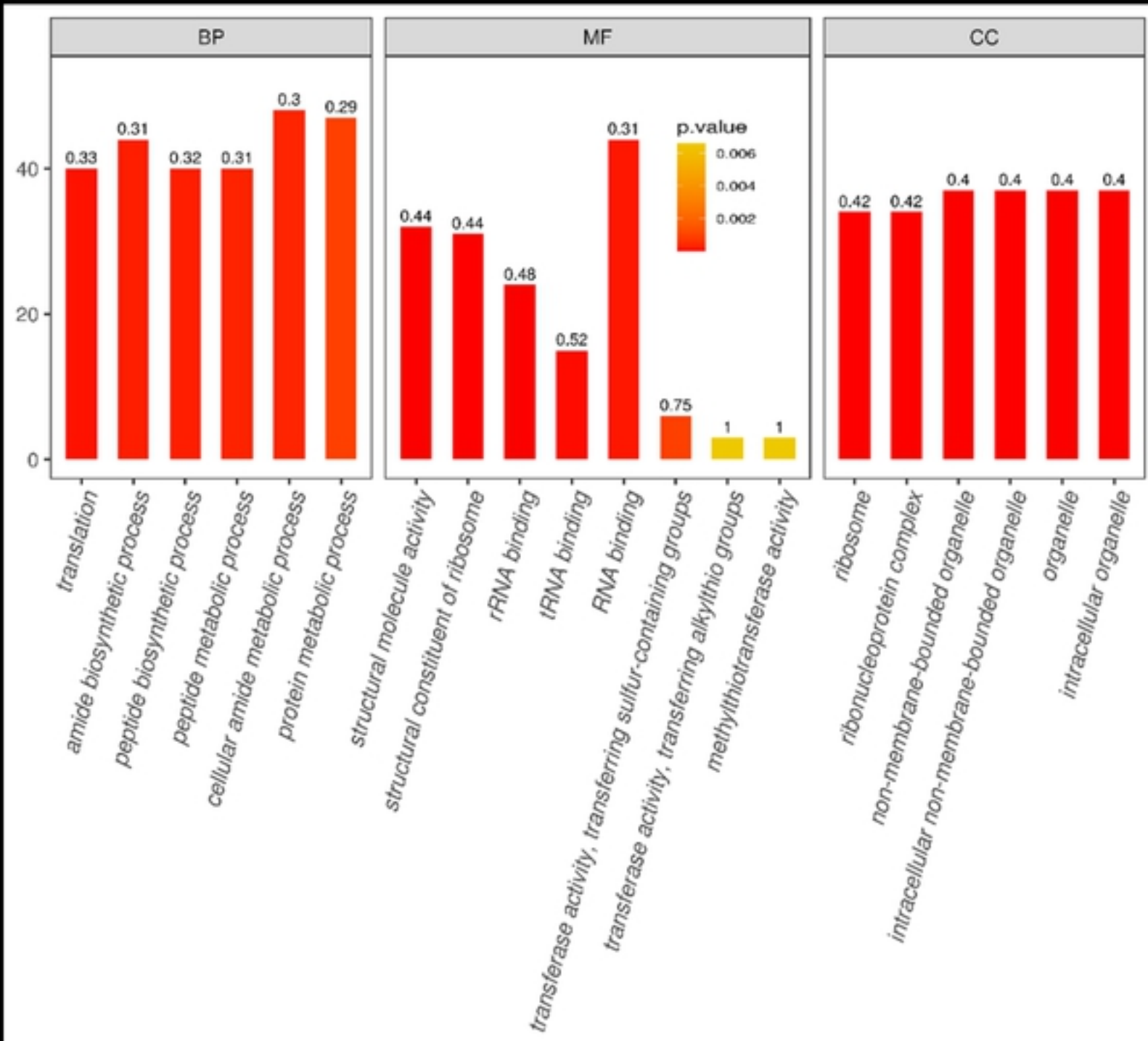


Fig 3

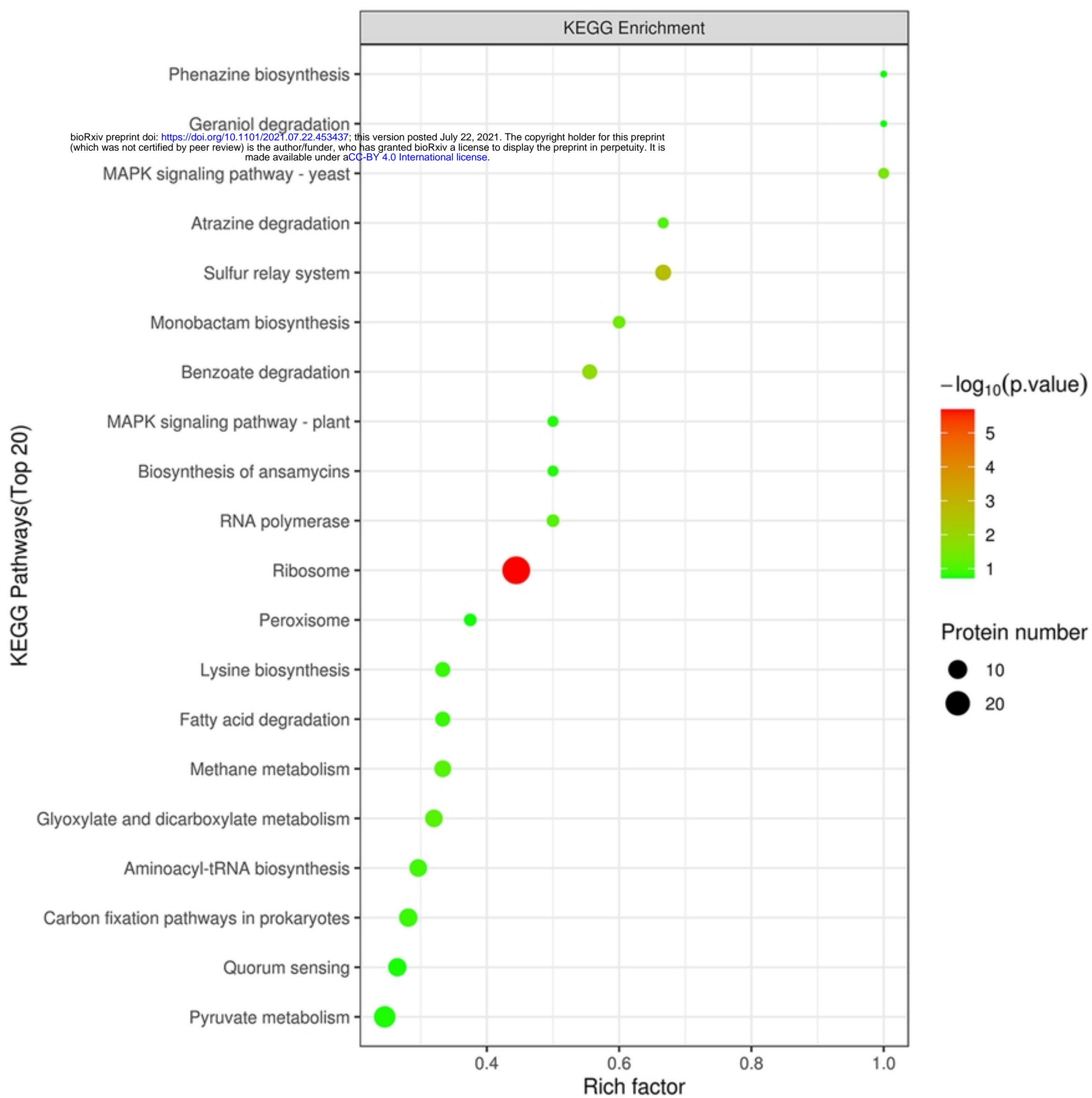
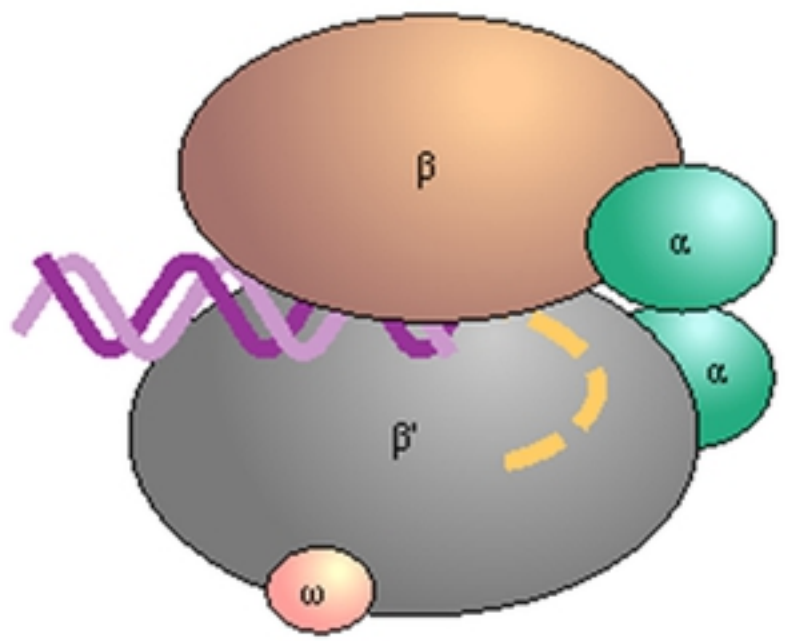
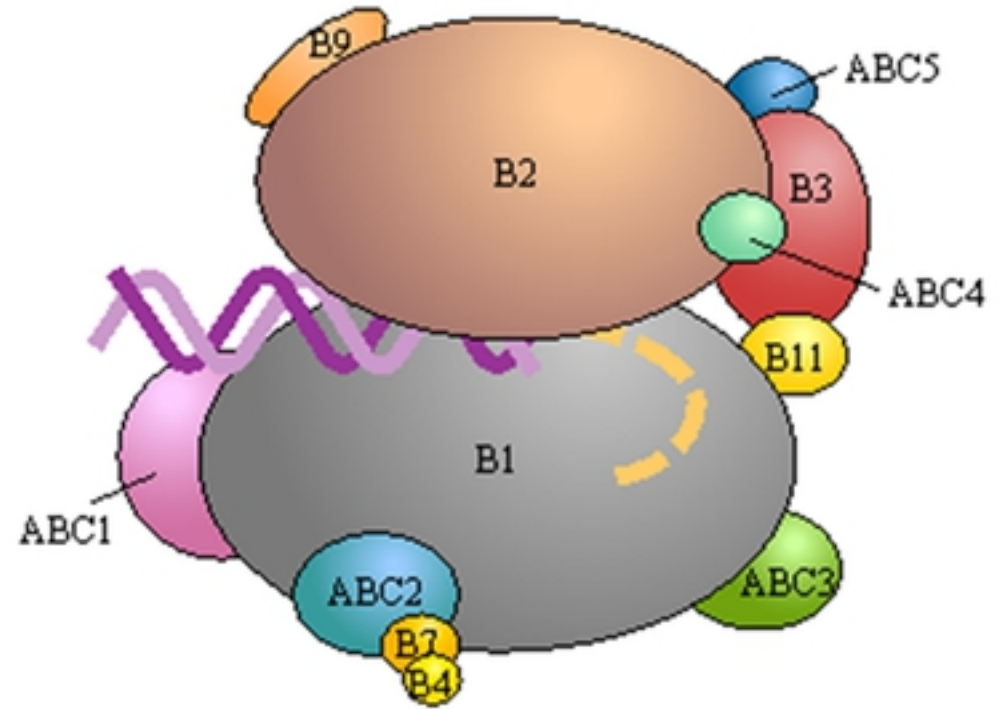


Fig 4

RNA POLYMERASE



RNA polymerase (*Thermus aquaticus*)

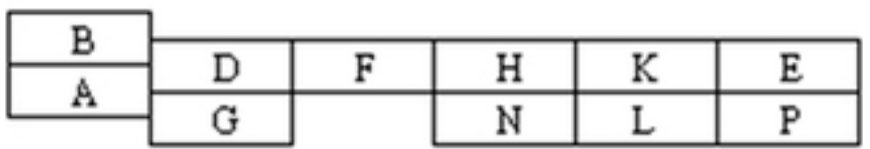


RNA polymerase II (*Saccharomyces cerevisiae*)

Bacterial



Archaeal



Eukaryotic Pol II

Core subunits

B2	B3
B1	B11

Pol II specific subunits

B4	B7	B9
----	----	----

Pol I, II, and III common subunits

ABC1	ABC2	ABC3
ABC4		ABC5

Eukaryotic Pol III

Core subunits

C2	AC2
C1	AC1

Pol III specific subunits

C3	C4	C11	
C25	C31	C34	C37

Eukaryotic Pol I

Core subunits

A2	AC2
A1	AC1

Pol I specific subunits

A12	A14	A34
A49		A43

Fig 5